



ELSEVIER

Journal of Chromatography A, 848 (1999) 365–374

JOURNAL OF  
CHROMATOGRAPHY A

# Use of artificial neural networks in capillary zone electrophoresis<sup>☆</sup>

Marta Farková, Eladia M<sup>a</sup>. Peña-Méndez<sup>1</sup>, Josef Havel\*

*Department of Analytical Chemistry, Faculty of Science, Masaryk University, Kotlářská 2, 611 37 Brno, Czech Republic*

Received 3 February 1998; received in revised form 21 March 1999; accepted 8 April 1999

## Abstract

The use of artificial neural networks (ANNs) for nonlinear modeling of symmetric and nonsymmetric peaks in capillary zone electrophoresis (CZE) and in optimization of CZE methods was studied. It was shown that ANNs can be used to estimate peak parameters and in combination with experimental design can be applied for efficient prediction of optimal separation conditions. The great advantage is that no use of the explicit model of the separation process and no knowledge of the physicochemical constants are needed. © 1999 Elsevier Science B.V. All rights reserved.

*Keywords:* Neural networks, artificial; Experimental design; Chemometrics; Peak shape; Optimization; Mathematical modeling; Computer simulation; Galanthamine; Alkaloids

## 1. Introduction

The use of chemometrics, especially multivariate data analysis, in any field of chromatographic techniques permits not only rapid and efficient optimization of the different chromatographic method developments, but chemometrics techniques are also of a great help in the study and interpretation of large chromatographic data sets containing a wide amount of information.

At this time, capillary electrophoresis (CE) shows

many advantages over conventional separation techniques like HPLC or GC. CE offers the advantages of high resolution, high separation efficiency and good reproducibility. However, the weak point of the method development in different modes of CE, such as capillary zone electrophoresis (CZE), gel electrophoresis (CGE), micellar electrokinetic capillary chromatography (MEKC), is to search of the optimal separation conditions; this procedure is sometimes tedious and the time-consuming part of the CE method development; high number of parameters affecting the separation, and further complications can arise from the mutual interaction of the parameters to be optimized.

The optimization procedure usually applied is a 'step-by-step' method, which can be called single variable approach (SVA). It involves a large number of independent analyses. Multivariate statistical methods, experimental design [1] and modeling techniques, have been used with the advantage in terms of reduction of the number of experiments,

<sup>☆</sup>Presented at the 11th International Symposium on High Performance Capillary Electrophoresis and Related Microscale Techniques, Orlando, FL, 1–5 February 1998.

\*Corresponding author. Tel.: +42-5-4112-9568; fax: +42-5412-11214.

*E-mail address:* havel@chemi.muni.cz (J. Havel)

<sup>1</sup>On leave from: Department of Analytical Chemistry, Nutrition and Food Science, University of La Laguna, La Laguna, Tenerife, Spain.

reduced analysis time and enhanced statistical evaluation of data. Experimental design is a planned interference in the natural order of events by the researcher, it does something more than carefully observe what is occurring. The most important aspect on experimental design is that it provides a strict mathematical framework for changing all pertinent factors simultaneously, and achieves this in the smallest number of experimental runs as possible.

Programs based on computer simulation of electrophoretic separations have been applied to various modes of CE and are described in several papers and textbooks [2]. Although the basic equations which describe such separations are well defined, there are some limitations in both of applicability to practical conditions and calculation speed, as well.

Limitations in information introduce errors in model predictions. New mathematical techniques such as artificial neural networks (ANNs) can reduce this difficulty. Neural network computing can be classified as a ‘soft model’. It is more robust like nonlinear regression models and can expose underlying relationships in a large data set of information using pattern recognition theory as for some recent applications, e.g. Ref. [3].

The theory of different networks has been reviewed by Zupan and Gasteiger [4]. Aleksander and Morton [5] defined ANN computing as ‘the study of networks of adaptable nodes, which through a process of learning from task examples, store experimental knowledge and make it available for use’. The node is the basic processing unit in neural networks. ANNs can consist of multiple layers of nodes arranged so that each node in one layer is connected with each node in the next layer. The strength of a connection between two nodes is called the weight.

Among different learning methods in neural network computing, the most popular method is the back propagation (BP) method and it is often used in analytical applications.

The theory of ANNs can be found in several reviews and papers, but in order to highlight some part of the neural computing necessary for a clear understanding of this work, we remark that the processing of information in ANNs can be divided into three levels: input layer, hidden layer, output layer. The node sums the product of each connection

weight ( $w_{jk}$ ) from a node  $j$  to the node  $k$  and input ( $x_j$ ) and the additional weight called the bias to get the value sum for the node  $k$ , Eq. (1)

$$\text{sum}_k = \sum_j x_j w_{jk} + \text{bias}_k \quad (1)$$

The  $\text{sum}_k$  of the weighted inputs is transformed with a transfer function, this function is used to get to the output level. Several functions can be used, function ‘sigmoid function’ is mostly applied.

The BP network ‘learns’ by adjusting its weights according to the error ( $E$ ), Eq. (2). The goal of training method is to change the weights between the layers in a direction that minimizes the error,  $E$ , it succeeds according to the steepest descent method, Eq. (3),

$$E = \frac{1}{2} \sum_p \sum_j (y_{p_j} - t_{p_j})^2 \quad (2)$$

where  $t$  is desired output and  $y$  is the output value,  $p$  is pattern number, and  $j$  means the number of the output nodes.

The current weight change is defined by Eq. (3):

$$\Delta w_{ij}(n) = -\eta \frac{\delta E}{\delta w_{ij}} \quad (3)$$

where  $\eta$  is a positive constant known as the ‘learning rate’ and  $\Delta w_{ij}(n)$  the current weight change for the weight  $w_{ij}$ . The weights are calculated in an iteration process from random values given initially. Gradient descent method can be enhanced by a ‘momentum term’ from the previous weight changes as, Eq. (4),

$$\Delta w_{ij}(n) = -\eta \frac{\delta E}{\delta w_{ij}} + \alpha \Delta w_{ij}(n-1) \quad (4)$$

where  $\alpha$  (momentum factor) is another constant.

The *lr*ate controls the update rate according to the new weights change and the *momentum* acts as stabilisator being aware of the previous weight changes. During the training procedure it is necessary to study the effect of the learning rate (*lr*ate) and *momentum* ( $\alpha$ ) in order to avoid overfitting problems. The learning process will stop when the network has reached a proper minimum error.

ANNs are applied in chemistry during the last years. An important field of their usage is also

optimization of separation processes in HPLC and ion chromatography [6–9].

A combination of experimental design and ANNs [10] has been recently shown to be a powerful tool in capillary electrophoresis to predict optimal separation conditions. Among the variables which might be determined during the optimization procedure in CE are peak parameters. In an ideal case, a Gaussian-shaped peak should be obtained, but in practice, the detected peaks frequently deviate more or less from the ideal Gaussian shape due to various dispersive effects. In fact, not only resolution,  $R_s$ , should be followed when searching for the optimal conditions. It is important also to follow effect of peak parameters, such as number of theoretical plates, peak width, symmetry, etc. The aim of this work was to continue in promising results obtained recently [10] and to apply ANNs in combination with experimental design for optimizing separation conditions taking into account also peak parameters.

To prove the experimental design–ANN approach, we used, as an example, CE determination of galanthamine. Galanthamine, an alkaloid of the common snowdrop, *Galanthus nivalis*, has been under consideration for symptomatic treatment of Alzheimer's disease. The compound is presently tested in Austria.

## 2. Experimental

The data were processed on a Pentium personal computer using back propagation neural networks (BPNNs), applying generalized delta rule, as included in the parallel distribution procedure (PDP) software package [11].

For all cases a feed-forward network was constructed by using the three layers ANN architecture and a systematic study was made for the influence of different neural parameters. The number of hidden nodes is an adjustable parameter and the optimal value was searched. Output values were scaled to be in the range [0, 1] (range of sigmoid transfer function outputs), and normalized outputs values were used for the output nodes. Together with the number of nodes in the hidden layer the other adjustable parameters were momentum factor, learning rate (*lr*ate), weights range, and the way of scaling of the

output. As the number of learning cycles, we found it optimal to use  $\leq 20\,000$  cycles.

To enhance the learning procedure in the back-propagation method the following techniques have been applied: (a) batching operation, (b) adaptive learning and momentum. In order to avoid overfitting, the performance of the neural network was tested every hundred or thousands of epochs during the training, and the weights for which the minimal RMS (root mean squares), Eq. (5), for the learning and test set were recorded.

$$\text{RMS} = \sqrt{\frac{\sum_{i=1}^N \sum_{j=1}^M (t_{ij} - y_{ij})^2}{M \cdot N}} \quad (5)$$

where  $t_{ij}$  is the element of the matrix ( $M \cdot N$ ) for the training or test sets, and  $y_{ij}$  is the element of the output matrix ( $M \cdot N$ ) of the neural network.

### 2.1. Experimental procedure and CE system

Galanthamine was obtained from Pharmachem (Bulgaria). The background electrolyte used for capillary electrophoresis of galanthamine was 20 mM sodium tetraborate from Lachema (Brno, Czech Republic). All other chemicals were of analytical grade purity and were also from Lachema. The water used was double distilled water from a quartz apparatus of Quartz Schmelze (Hanau, Germany). Buffer solutions were filtered through glass S4 filters of Kavalier (Votice, Czech Republic) and degassed before use.

Electrophoretic measurements were carried out using SpectraPhoresis 1000 of Thermo Bioanalysis Corp. (San José, CA, USA). A fused-silica capillary 42.7 cm (35.9 cm to the detector)  $\times$  0.57  $\mu\text{m}$  of Composite Metal Services (The Chase, Hallow, UK) was used. Detection at 210 nm and/or high speed scan of the spectra was used throughout the work. The samples were injected hydrodynamically (using vacuum 10.3 kPa relative to ambient pressure). All the analysis were carried out at 25°C.

The pH was measured using Radelkis OP-208 Precision Digital pH meter of Radelkis (Budapest, Hungary) and a Radelkis pH sensitive, combined glass–calomel electrode of Radelkis.

## 2.2. Simulation procedures

Symmetric peaks were simulated using Lorentz function,  $y = (\beta_1/[1 + \beta_2(x - \beta_3)^2])^2$ , where  $\beta_1 = 5, 10$  and  $15$ ;  $\beta_2 = 0.01, 0.1$  and  $0.9$ ;  $\beta_3 = 30$  to  $70$ . Nonsymmetric peaks were modeled using either the Weibull function,  $y = (cx^{c-1}/\delta^c) \exp[-(x/\delta)^c]$ , where  $c = 2$  to  $10$  and  $\delta = 20$  to  $85$ , or using the Gaussian-exponential function

$$y = a \frac{\sigma_G}{\tau} \sqrt{2} \exp \left[ 1/2 \left( \frac{\sigma_G}{\tau} \right)^2 - \frac{x - t_G}{\tau} \right] \int_{-\infty}^{z/\sqrt{2}} \exp(-t^2) dt \quad (6)$$

where  $z = (x - t_G)/\sigma_G - \sigma_G/\tau$ ;  $A = 1$ ;  $t_G = 50, 62, 68$  and  $73$ ;  $\sigma_G = 1.2, 1.8$  and  $2.7$ ;  $\tau = 5.4, 6.8, 7.7$  and  $8.4$ . It is well known that most of the peaks in chromatographic methods possesses just this Gaussian-exponentially modified shape ( $A$  is area of the peak,  $t_G$  is retention time,  $\sigma_G$  standard deviation and  $\tau$  the time constant of the exponential function).

## 3. Results and discussion

### 3.1. Case 1: Determination of the parameters of an electrophoretic peak

Simulated data for either the symmetric or nonsymmetric peaks, respectively, were divided into the training and test sets. BP neural networks having three layers were created. During the training the optimization of the adjustable parameters, learning rate, momentum, number of hidden nodes, and number of learning cycles was carried out by systematically varying each of the parameters until the best network performance was achieved. As starting set of network parameters used in order to achieve the minimal total sum of squares of residuals ( $tss$ ) was: (a) for symmetric peaks  $lrate = 0.006$ ,  $wrange = 0.9$ , (b) for nonsymmetric peaks for Weibull function  $lrate = 0.005$ ,  $wrange = 0.9$ , (c) for nonsymmetric peaks for Gaussian-exponential function  $lrate = 0.00001$ ,  $wrange = 0.9$ .

Symmetric peaks were simulated using Lorentz function. The corresponding data set is shown in Fig. 1a. From the total data set, 35 patterns were chosen

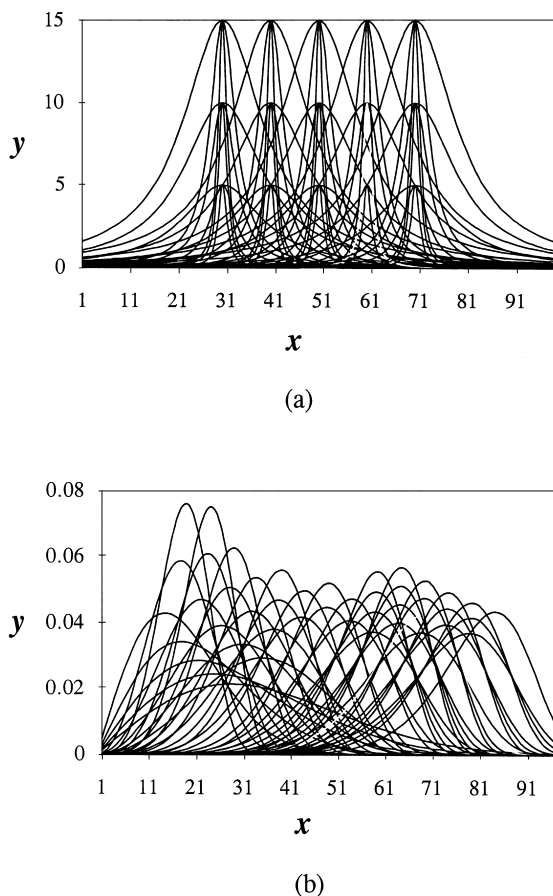


Fig. 1. (a) Simulated peaks of Lorentz function shape. (b) Simulated peaks of Weibull function shape.

for the training and 10 patterns for the test set. In this case, 22:17:3 architecture was found to be optimal (Fig. 3a).

Nonsymmetric peaks were simulated using Weibull function and the data set is shown in Fig. 1b. The training set consisted of 35 patterns and 10 patterns were used as a test set. In this case 14:24:2 architecture was found to be optimal (Fig. 3b).

For nonsymmetric peaks which were simulated using the Gaussian-exponential function, part of the data set (total 46 curves) are shown in Fig. 2. Training set consisted of 36 patterns and a test set of 10 patterns. For ANN we have defined the INPUT represented by 22 values of  $(x, y)$  pairs for each curve and as OUTPUT three parameters of the peaks

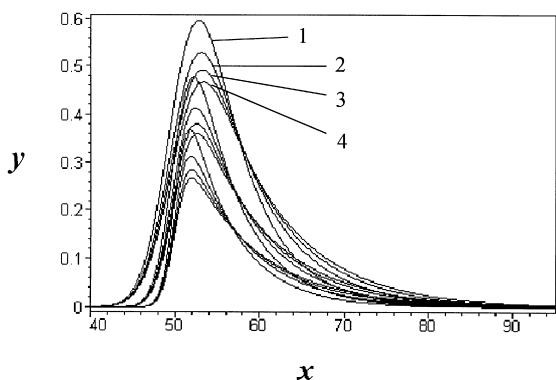


Fig. 2. Simulated peaks possessing Gaussian-exponential function form (cf. Eq. (6)) (parameters  $t_G$ ,  $\sigma_G$  and  $\tau$  of the curves 1–4 are 1: 50, 2.7 and 5.4; 2: 50, 2.7 and 6.8; 3: 50, 2.7 and 7.7; 4: 50, 2.7 and 8.4).

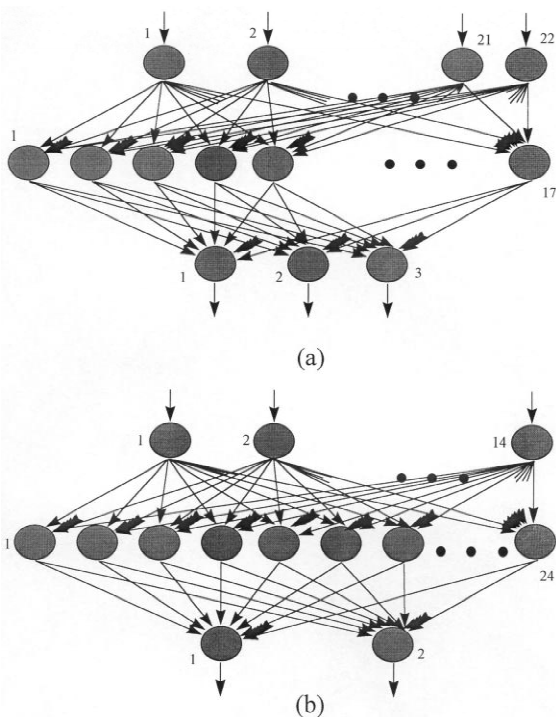


Fig. 3. Different ANN architectures used for modeling. (a) ANN architecture (22:17:3) for symmetric peaks (Lorentz); (b) ANN architecture (14:24:2) used for unsymmetric peaks (Weibull).

( $t_G$ ,  $\sigma_G$ ,  $\tau$ ) were used. The parameters were normalized into  $t'_G = t_G/75$ ,  $\sigma'_G = \sigma_G/3$ ,  $\tau' = \tau/9$  to satisfy the requirements of the PDP program.

The first stage of the calculation was again to find an optimal ANN structure. The search for the ANN structure was done using TRAINING SET and the optimal performance was obtained for 22:6:3 architecture.

[Remark: learning rate (*lr*ate value) attempts to keep the learning step-size as large as possible. The use of an adaptive learning rate leads to a lower training rate. But if its value is set too high, the error in prediction soon starts to oscillate or grows up.]

Results for the test sets for both, symmetric and nonsymmetric peaks, are given in Fig. 4. In all cases it is evident that partial sum of squares of residuals

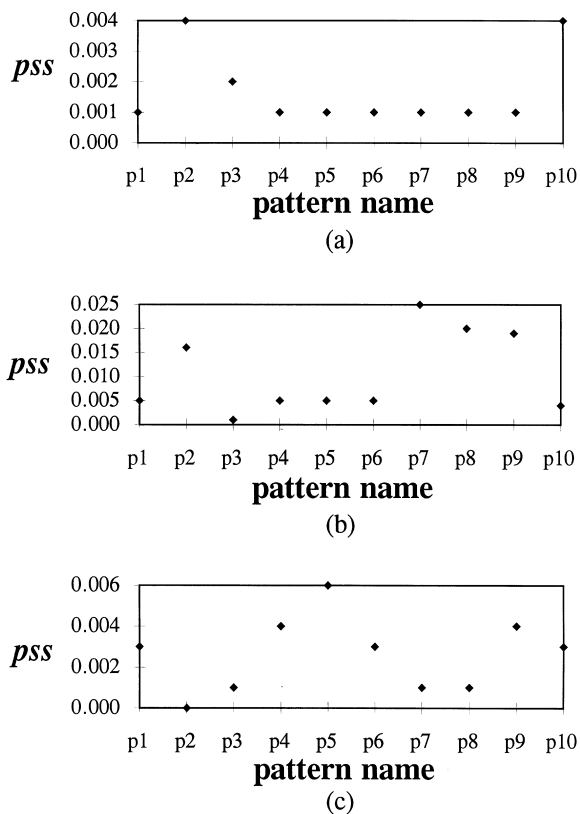


Fig. 4. Quality of the ANN models for different shapes of the electrophoretic peaks. The values of *pss* for the test sets: (a) Lorentz function; (b) Weibull function; (c) Gaussian-exponential function. *pss* is the partial sum of squares.

( $pss$ ) is small which is evidence of a very good prediction obtained by ANN.

### 3.2. Case 2: Optimization of separation conditions in capillary electrophoresis

CZE was applied by Massart et al. [12], for the determination of the mono-, di- and trivalent cations. The authors applied for the optimization central composite design (CCD) and modeling technique using an empirical model given by Eq. (7), which relates the ion mobility ( $\mu_{M_i}$ ) with the complexing agent 18-crown-6 concentration ( $c_{crown}$ ) and methanol ( $c_{MeOH}$ ) concentration

$$\mu_{M_i} = k_0 + k_1 c_{crown} + k_2 c_{crown} + k_3 c_{MeOH} + k_{22} c_{crown}^2 \quad (7)$$

where  $k$  values represent the empirical parameters given in Table 1.

There is an important relation between the resolution ( $R_s$ ) and  $N$  (number of theoretical plates) and electrophoretic mobilities  $\mu_a$  and  $\mu_b$ , Eq. (8),

$$R_s = [(N)^{1/2}/4] \{(\mu_a - \mu_b)/(\mu_{av} - \mu_{eo})\} \quad (8)$$

where  $\mu_a$  and  $\mu_b$  are the electrophoretic mobilities of two neighbouring metal cations ( $\mu_a > \mu_b$ ), and  $\mu_{av}$  and  $\mu_{eo}$  are average and electroosmotic mobilities, respectively.

In the same way as before, we have simulated response resolution surface for three of the cations in this paper, see Fig. 5. The surface represents the response for the separation conditions of three different cations. The value of  $\Delta\mu_{\min}$  ( $\Delta\mu_{\min}$  is the minimum of the values  $|\mu_{M_1} - \mu_{M_2}|$ ,  $|\mu_{M_1} - \mu_{M_3}|$  and

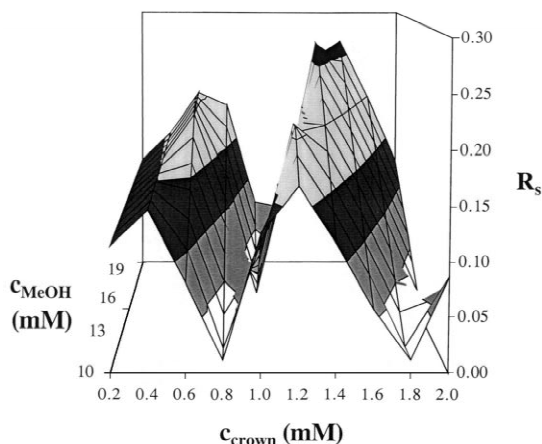


Fig. 5. Simulated three-dimensional response resolution surface (Case 2) for the electrophoretic separation of three cations.

$|\mu_{M_2} - \mu_{M_3}|$ ) was used as the criterion to search for the optimum experimental conditions,  $R_{s\min} = \Delta\mu_{\min}$ . The empirical values,  $k$ , assumed for Eq. (7), are given in Table 1. They were used to calculate the values  $\mu_{M_1}$ ,  $\mu_{M_2}$  and  $\mu_{M_3}$ . The concentration of methanol was varied from 10 to 20% and 18-crown-6 concentration changed from 0.5 to 2.0 mM.

### 3.3. Case 2, Part 1: Search of ANN optimal structure

Simulated values of the resolution were rearranged to present two inputs ( $c_{crown}$  and  $c_{MeOH}$ ) and one output (resolution,  $R_s$ ). The data set was divided into a training set and a test set.

BP neural networks having three layers were created. During the training the optimization of the adjustable parameters, learning rate, momentum, number of hidden nodes, and number of learning cycles was carried out by systematically varying each of the parameters until the best network performance was achieved. In this work the starting set of the parameters used in order to achieve the minimal  $tss$  value was for  $lrate = 0.05$ ,  $wrange = 0.9$  and cycles  $\leq 20\,000$ .

The training of ANNs was done for several different ANN architectures and, finally, the optimal performance was found for the architecture 2:7:1. The residuals obtained for the training set are shown

Table 1

Empirical constants used to calculate electrophoretic mobilities with Eq. (7)

Empirical constants in Eq. (7)	$M_1$	$M_2$	$M_3$
$k_0$	0.10000	-0.00500	0.00500
$k_1$	0.00300	0.00350	0.00400
$k_2$	0.02000	0.02100	-0.02000
$k_3$	0.01100	-0.01000	0.01000
$k_{22}$	-0.10000	-0.00100	-0.30000

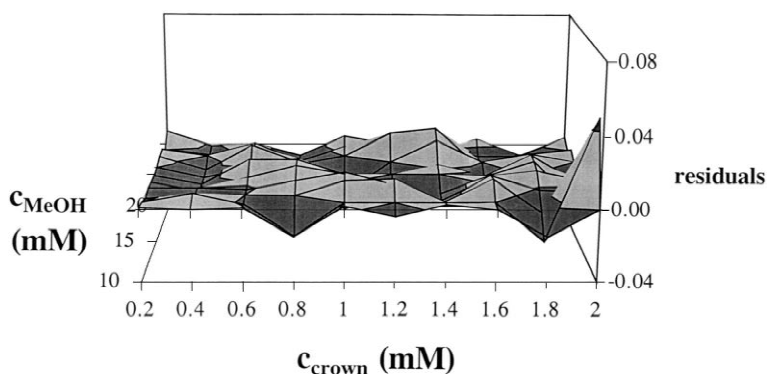


Fig. 6. Quality of the ANN modeling for the electrophoretic separation of three cations. The residuals,  $R_{\text{exp}} - R_{\text{pred}}$ , for the training set (Case 2).  $R_{\text{exp}}$  is the experimental value of the resolution, while  $R_{\text{pred}}$  is the value predicted by the ANN approach.

in Fig. 6. It can be seen that even for such a complicated response function a very good fit was obtained.

### 3.4. Case 2, Part 2: The prediction of optimum CZE separation using a combination of experimental design and artificial neural network

Two-level CCD was used and the following strategy applied:

*Step 1.* The ANN was trained and in this way the corresponding weights ( $w_{ij}$ ) were obtained; the training set (nine points) is shown in Table 2 (bold black numbers).

*Step 2.* BP program has been applied and the

prediction performed. The weights ( $w_{ij}$ ) obtained in Step 1 were used to predict the values of the test set, signed by italic numbers, Table 2. Fig. 7 shows the comparison between predicted  $R_s$  values as obtained with ANN and experimental values. It can be seen that the predicted values of the resolution for Pattern No. 3 (p3), Fig. 7, is greater than the  $R_s$  value obtained for the other points used in the test set. It can be concluded that it would be useful to realize new ‘experiments’ around this point.

*Step 3.* The other experimental design (underlined numbers, Table 2) was applied in the region centered around the greatest value obtained in Step 2, and the quality of the fit achieved in this second training procedure was then excellent.

Table 2  
Resolution values used to study the performance of ANN

$C_{\text{MeOH}}$ (mM)	$C_{\text{crown}}$ (mM)										
	10	11	12	13	14	15	16	17	18	19	20
0.2	0.1145	0.1155	0.1165	0.1175	0.1185	0.1195	0.1205	0.1215	0.1225	0.1235	0.1245
0.4	0.1465	0.1475	0.1485	0.1495	0.1505	<b>0.1515</b>	0.1525	0.1535	0.1545	0.1555	0.1565
0.6	0.0810	0.1010	0.1210	0.1410	0.1610	0.1810	0.2005	0.2015	0.2025	0.2035	0.2045
0.8	0.0109	0.0091	<b>0.0291</b>	0.0491	0.0691	0.0891	<i>0.1091</i>	0.1291	<b>0.1491</b>	0.1691	0.1891
1	0.1268	0.1068	0.0868	0.0668	<i>0.0468</i>	<u>0.0268</u>	<u>0.0068</u>	<u>0.0133</u>	0.0333	0.0533	0.0733
1.2	<b>0.1680</b>	0.1890	0.2100	0.2065	0.1865	<b>0.1665</b>	0.1465	0.1265	0.1065	0.0865	<b>0.0665</b>
1.4	0.1163	0.1373	<i>0.1583</i>	0.1793	<u>0.2003</u>	0.2213	<i>0.2423</i>	0.2633	<u>0.2702</u>	0.2502	0.2302
1.6	0.0567	0.0777	<b>0.0987</b>	0.1197	<u>0.1407</u>	0.1617	0.1827	0.2037	<b>0.2247</b>	0.2457	0.2667
1.8	0.0108	0.0102	0.0312	0.0522	<i>0.0732</i>	<u>0.0942</u>	0.1152	<u>0.1362</u>	0.1572	0.1782	0.1992
2	0.0863	0.0653	0.0443	0.0233	0.0023	<b>0.0188</b>	<u>0.0398</u>	0.0608	0.0818	0.1028	0.1238

Subset of the resolution data to train the network. Numbers marked (bold, underlined, or italic) mean points of the experimental design used to search the maximum of the response surface as shown in Fig. 5.

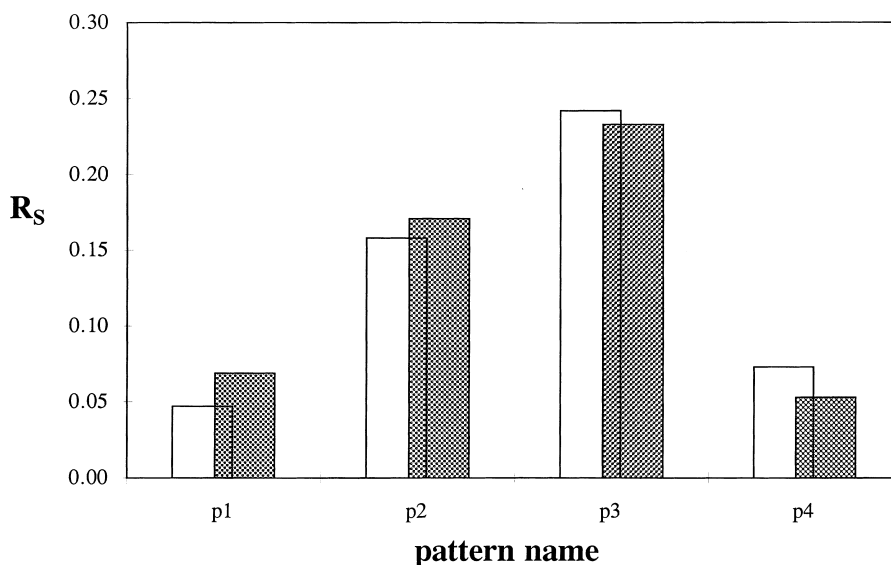


Fig. 7. Comparison between ANN predicted  $R_s$  data (▨) and simulated  $R_s$  values (□) for the test set in the second step of optimization (Case 2).  $R_s$  is resolution.

Thus, it was shown that by adding new experiments no further improvement was reached, which was evidence that the optimum has already been found.

### 3.5. Case 3: Prediction of the optimal separation conditions

To compare results of MVA versus SVA, in this part of the work the optimization of CZE experiments was achieved in two different ways: (1) step-by-step, (2) using a multivariate approach and applying a combination of experimental design–ANN.

Data sets were obtained from the experimental conditions and electropherograms of the compounds provide the necessary features to test the utility of the various parameters in the optimization procedure. For each case the performance of the neural network, searching the best architecture has been made in the same way as in Case 1. At the same time, the procedure for applying experimental design–ANN was the same as above.

### 3.6. Case 3, Part 1: Optimization of galanthamine determination using a combination of experimental design and ANN

Pokorná et al. [13] have developed a CZE method for determination of galanthamine.

We have compared the results obtained by SVA during the optimization procedure of galanthamine with those obtained applying experimental design–ANN.

Selection of a specific type of designs depends primarily on both the nature and the extent of the information we want to obtain. To summarize the MVA three-factor central composite design was selected, a data set containing 18 patterns was divided into the training and the test set, and an architecture 2:7:1 was selected for the neural.

The experimental design–ANN approach has been applied and the predicted values for pH, injection time and separation voltage are presented in Table 3. These ‘best’ conditions were run in the CE machine and the resulting electropherogram is shown in Fig. 8. This figure is the overlay of two electropherograms – electropherograms for galanthamine CZE



Table 3

Comparison of optimal separation conditions and peak parameters obtained by single variable approach and multivariate approach

Variable	Single variable approach	Multivariate approach
Optimal separation conditions		
pH	8.3	7.0
Injection time	30 s	5 s
Separation voltage	10 kV	22 kV
Peak Parameters		
Migration Time	4.29 min	1.69 min
Area	43 950 $\mu$ AU s	108 370 $\mu$ AU s
Height	18.40 mAU	122.95 mAU
Number of theoretical plates	80 470	92 010

determination under optimal conditions obtained by SVA or the MVA approach. Better separation conditions have been obtained and the 'best' parameters of the galanthamine peak obtained are presented in Table 3.

These results demonstrate that the MVA optimization strategy using experimental design-ANN gets better results and is consuming less experimental work than SVA.

#### 4. Conclusions

ANNs with suitable structure can, after a proper learning stage, be used to predict (i) peak parameters for symmetrical and/or nonsymmetrical peaks of any shape, (ii) optimal separation conditions, without any necessity to have an explicit model.

A combination of experimental design and ANNs with backpropagation algorithm allows to predict the

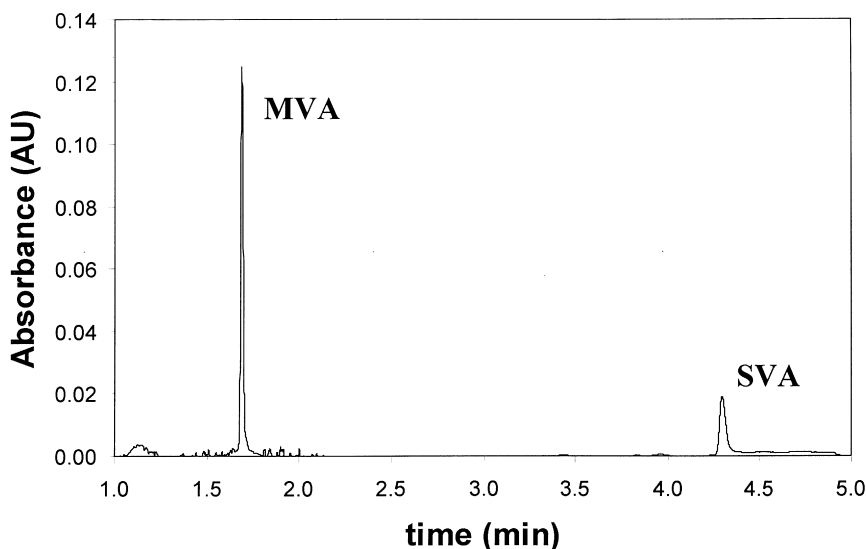


Fig. 8. Comparison of electropherograms for galanthamine ( $c = 1 \mu\text{g/ml}$ ) CZE determination in aqueous solution under optimal conditions obtained by the SVA or MVA approach (overlay of two different electropherograms). Conditions – SVA: pH=8.3, injection time=30 s, separation voltage=10 kV, MVA: pH=7.0, injection time=5 s, separation voltage=22 kV.

optimal separation conditions using a lower number of experiments.

### Acknowledgements

We wish to acknowledge Grant Agency of Czech Republic, grant No.203/96/0478 for support of this work. Masaryk University is thanked for a post-doctorate scholarship and University of La Laguna for partial financial support to one of us (E.M.P.). Mrs. Lenka Pokorná is thanked for her technical assistance.

### References

- [1] S.N. Deming, S.L. Morgan, *Experimental Design: A Chemometric Approach*, Elsevier, Amsterdam, New York, 1987.
- [2] J.C. Reijenga, E. Kenndler, *J. Chromatogr. A* 659 (1994) 403–415, 417–426.
- [3] M. Blanco, J. Coello, H. Iturriaga, S. Maspoch, M. Redón, J.F. Rodríguez, *Quím. Analítica* 15 (1996) 266–275.
- [4] J. Gasteiger, J. Zupan, *Neural Networks in Chemistry*, *Angew. Chem.* 32 (1993) 503–527.
- [5] I. Aleksander, H. Morton, *An Introduction to Neural Computing*, Chapman and Hall, London, 1990.
- [6] E. Marengo, M.C. Gennaro, S. Angelino, *J. Chromatogr. A* 799 (1998) 47–55.
- [7] T.D. Booth, K. Azzaoui, I.W. Wainer, *Anal. Chem.* 69 (1997) 3879–3883.
- [8] G. Sacchero, M.C. Bruzzoniti, C. Sarzanini, E. Mentasti, H.J. Metting, P.M.J. Coenegracht, *J. Chromatogr. A* 799 (1998) 35–45.
- [9] J. Havel, J.E. Madden, P.R. Haddad, *J. Chromatogr. A* (1998) in press.
- [10] J. Havel, E.M. Peña-Méndez, A. Rojas-Hernández, J.-P. Doucet, A. Panaye, *J. Chromatogr. A* 793 (1998) 317–329.
- [11] J.L. McClelland, D.E. Rumelhart, *Explorations in Parallel Distributed Processing*, MIT Press, Cambridge, 1988, A Bradford Book.
- [12] Q. Yang, J. Smeyers-Verbeke, W. Wu, M.S. Khots, D.L. Massart, *J. Chromatogr. A* 688 (1994) 339.
- [13] L. Pokorná, A.L. Revilla, J. Havel, J. Patočka, *Electrophoresis* (1999) in press.